Biosensors and Bioelectronics 49 (2013) 442–449

Contents lists available at SciVerse ScienceDirect

Biosensors and Bioelectronics

journal homepage: www.elsevier.com/locate/bios

Isothermal detection of multiple point mutations by a surface plasmon resonance biosensor with Au nanoparticles enhanced surface-anchored rolling circle amplification

Yang Xiang*, Kun Deng, Han Xia, Chunyan Yao, Qinghai Chen, Liqun Zhang, Zhiyong Liu, Weiling Fu*

Laboratory of the Clinical Experimental Base of Biosensor and Microarray, and the Center of Molecule and Gene Diagnosis, Southwest Hospital, Third Military Medical University, Chongqing 400038, PR China

ARTICLE INFO

Article history:
Received 19 January 2013
Received in revised form
23 April 2013
Accepted 23 April 2013
Available online 25 May 2013

Keywords:
Surface plasmon resonance
Rolling circle amplification
Au nanoparticles
Multiplex mutation detection
Multidrug-resistant *Mycobacterium tuberculosis*

ABSTRACT

In this study, we developed a surface plasmon resonance (SPR) DNA biosensor method using surface-anchored rolling circle amplification (RCA) and Au nanoparticles modified probes (AuNPs) to isothermally detect multiple point mutations associated with drug-resistance in multidrug-resistant *Mycobacterium Tuberculosis* (MDRTB). A set of probes contains an allele-specific padlock probe (PLP), a capture probe and an AuNPs. The linear PLPs, circularized by ligation upon the recognition of the point mutation on DNA targets, hybridize to the capture probes via the specific tag/anti-tag recognition. Upon recognition each point mutation is identified by locating into the corresponding channel on the chip. Then the immobilized primer (capture probe)–template (circular PLP) complex are amplified isothermally as RCA and further amplified by AuNPs. The RCA products immobilized on the chip surface cause great SPR angle changes consequently. The 5 pM synthetic oligonucleotides and 8.2 pg uL^{-1} of genomic DNA from clinical samples can be detected by the method. The positive mutation detection is achieved with a wild-type to mutant ratio of 5000:1. The method was demonstrated by targeting five clinically meaningful mutations in MDRTB. Thirty clinical samples were identified and they were in good agreement with the results from sequencing.

1. Introduction

Tuberculosis (TB), caused by *Mycobacterium tuberculosis*, remains a global pandemic resulting in significant morbidity and mortality, responsible for 1.4 million deaths and 8.7 million new cases in 2012 (World Health Organization, 2012). A steady drug-resistant increase of *M. tuberculosis* has threatened TB control world-wide, despite advancements in the diagnosis and treatment of TB over the years. The multidrug-resistant *M. tuberculosis* (MDRTB) is defined as being resistant to at least isoniazid and rifampin. The emergence and spread of MDRTB pose an upward trend and represent an increasing public health problem due to the HIV/AIDS pandemic which has intensified the threat of TB (Diedrich and Flynn, 2011). Resistance to anti-TB drugs is related to mutations affecting the function and/or expression of chromosome-encoded targets (Ramaswamy and Musser, 1998). Conventional culture-based method or sequence analysis is reliable but relatively time consuming, laborious and expensive (Veigas et al., 2010). Therefore, the development of a simple, sensitive and low-cost method is important for the rapid detection of drug-resistance; it is a timely and effective way to diagnose and manage TB patients, especially MDRTB cases.

SPR biosensor is a flow-through biosensor technology measuring very small changes in refractive index on a noble metal surface when mass bond to the surface (Homola, 2008). Because of its high sensitivity of optical transducer, convenient operation and real-time monitoring, it is applied to study variety of bimolecular interactions including DNA, RNA, protein and peptides (Mannelli et al., 2006; Chu et al., 2007; Garcia and Goodman, 2008; Mitchell and Lowe, 2009). In a SPR biosensor assay, the change of the refractive index on the gold film correlates with the amount of analyte bound to the film (Bailey et al., 2009). In most of SPR-based DNA detection with high sensitivity, nucleic acid amplification is adopted to amplify analyte mass, especially polymerase chain reaction (PCR) (Jin et al., 2009; Wang et al., 2010, 2011). However, the non-specific amplification from complicated thermal circling step, non-compatibility with on-chip amplification and increase of detection cost are still problems to be considered.

Focusing on the development of isothermal amplification methods, such as RCA (rolling circle amplification), Lamp (loop-mediated isothermal amplification) and HCR (hybridization chain reaction), emerges for its simplicity in the detection of nucleic acids (Zhang et al., 2009; Lee et al., 2010; Niu et al., 2010). RCA has shown its attraction due to the specificity and multiplexing

* Corresponding authors. Tel.: +86 236 875 4429; fax: +86 236 546 0909.
E-mail addresses: xyang_@hotmail.com (Y. Xiang), weilingfu@yahoo.com (W. Fu).

0956-5663/$ - see front matter © 2013 Published by Elsevier B.V.
http://dx.doi.org/10.1016/j.bios.2013.04.044

besides simplicity (Banér et al., 2001; Schweitzer and Kingsmore, 2001). In a typical ligation-rolling circle amplification (L-RCA) reaction, once the perfect hybridization of the linear PLPs target-specific region occurs with the targets, the ligase seals the nick and circularizes the probe. RCA is followed by mimicking bacteriophage replication in vivo (Zhong et al., 2001). After annealing of a forward primer to its complementary sequence on the circular PLP, the DNA polymerase with displacement activity extends this forward primer along the circular PLP for hundreds of rounds leading to linear amplification. Up to 10^5 tandem repeats of the PLP are generated under a constant temperature (Banér et al., 1998). The L-RCA by ligase relies on base pairing principle which requires perfect complementarity on the ligation nick. It not only forbids the mismatch but also has a low occurrence of false positive results when compared to PCR (Lizardi et al., 1998). When used as a signal amplification method, this property enabled high multiplexing without interference, direct amplification on solid phase and precise product localization (Hatch et al., 1999). Moreover, RCA amplifies the circular PLP only, without accumulation of target templates over time, which minimizes the risk of contamination and the potential biohazard. Besides, the nanoparticle amplification method using the sandwich hybridization of probes functionalized Au nanoparticles further enhances the signal amplification of RCA. The Au nanoparticles binding to the RCA products act as the electromagnetic field coupling with the Au film to enhance the plasmon resonance excited by the incident light, and improve the transduction of small changes in refractive index on the chip surface media, thus improving the sensitivity of SPR biosensor (Petryayeva and Krull, 2011).

The key challenges in multiplex mutations parallel detection include the design and selection of specific probes, precise localization of multiplexing probes and unbiased signal amplification. In this work, we presented a new strategy using the multi-channel SPR biosensor array combined with the surface-anchored RCA and Au nanoparticles signal amplification technique to identify multiple point mutations in parallel. A multiplex assay was established to target five mutations in MDRTB. The circular PLPs mixture generated by the ligation in solution was added to the detection well to hybridize with the capture probes via the specific tag/anti-tag sequence. This process divides one multiplex assay into several singleplex reactions in corresponding addresses on a sensor chip. Surface-anchored RCA and AuNPs were followed to amplify the hybridization signal twice and achieve low-abundant point mutation detection. The sensitivity and specificity of the SPR method were evaluated, and the application was also tested in clinical samples.

2. Materials and methods

2.1. Materials

All HPLC-purified oligonucleotide were synthesized by Sangon Biotech (Shanghai, China) (Table 1). Phi29 DNA polymerase, exonuclease I and exonuclease III were purchased from New England Biolabs (USA). The mixture of deoxyribonucleosides (dNTPs) and HhaI restriction enzyme was from Fermentas (USA). *Escherichia coli* DNA ligase and bovine serum albumin (BSA) were from Takara (Dalian, China). Mercaptoethanol and dimethyl sulfoxide were from

Table 1
Oligonucleotides used in this study.

Oligonucleotides	Sequence(5′–3′)	
Padlock probes	katG315 (G→C)	p*TGGTGATCGCGTCCT*GTATACGCTTCTTCGGTGCCCATGCGC**TGCG-ACCT-CAGC-ATCG-ACCT**GTCTA*GACCTCGATGCAGG*
	inhA-15 (C→T)	p*TCTCGCCGCGGCCGGG*TATACGCTTCTTCGGTGCCCATGCGC**GACC-ACCT-TGCG-ATCG-GGTA**GTCTA*CAGACAACCTATCA*
	rpoB526 (C→T)	p*GGTCAACCACGACAGCGG*TATACGCTTCTTCGGTGCCCATGCGC**TGCG-GGTA-CAGC-ACCT-ACCT**GTCTA*GTCGGCGCTGTA*
	embB306 (A→T)	p*GCACAGGATGTAGCCG*TATACGCTTCTTCGGTGCCCATGCGC**CAGC-ATCG-GACC-GGTA-ATCG**GTCTA*GACTCGAGCCAA*
	rpsL43 (A→G)	p*TCGGAGTGGTGGTGTAC*GTATACGCTTCTTCGGTGCCCATGCGC**GACC-GGTA-TGCG-ACCT-GGTA**GTCTA*GAGTTCGGCTTCC*
Capture probes	Tag1 (katG315)	HS-$(CH_2)_6$-$(T)_{20}$AGGT-CGAT-GCTG-AGGT-CGCA
	Tag2 (inhA-15)	HS-$(CH_2)_6$-$(T)_{20}$TACC-CGAT-CGCA-AGGT-GGTC
	Tag3 (rpoB526)	HS-$(CH_2)_6$-$(T)_{20}$AGGT-AGGT-GCTG-TACC-CGCA
	Tag4 (embB306)	HS-$(CH_2)_6$-$(T)_{20}$CGAT-TACC-GGTC-CGAT-GCTG
	Tag5 (rpsL43)	HS-$(CH_2)_6$-$(T)_{20}$TACC-AGGT-CGCA-TACC-GGTC
AuNPs		HS-$(CH_2)_6$-CGCTTCTTCGGTGCCCAT
Target sequences	katG315 (W)	TGGCACCGGAACCGGTAAGGACGCGATCACCAGCGGCATCGAGGTCGTATGGACGAA
	katG315 (ACC)	TGGCACCGGAACCGGTAAGGACGCGATCACCACCGGCATCGAGGTCGTATGGACGAA
	inhA-15 (ATG)	taccgatttcggcccggccgcggcgagaTgataggttgtcggggtgactg
	rpoB526 (TAC)	tcggggttgacccacaagcgccgactgtTggcgctggggcccggcggtct
	embB306 (GTG)	GTCGGACGACGGCTACATCCTGGGCTTGGCCCGAGTCGCCGACCACGCCG
	rpsL43 (AGG)	gcacccgcgtgtacaccaccactccgaGgaagccgaactcggcgcttcgg

The allele-specific site in PLPs and the mutation site in targets are at the border. The italic bases in PLPs match the sequence underlined in targets, while the hyphened bold bases (tag-sequence) match the sequence in capture probes, and "*p*" represents a phosphate at 5′ end for ligation. The nucleotides substitutions within target-specific region are in gray shading. The capture probes and AuNPs are modified with thiol group at 5′ end for immobilization on the gold film.

Sigma-Aldrich (St. Louis, MO, USA). Au nanoparticles synthesized by citrate reduction of $HAuCl_4$ solution with an average diameter of 15 nm were obtained from JY Biotech (Shanghai, China). Phosphate buffered saline (PBS) (0.15 M NaCl, 10 mM phosphate, pH 7.2) and Piranha solution (H_2O_2:H_2SO_4=1:3) were prepared. All chemicals employed were of analytical degree. Standard bacterial strains *M. tuberculosis* (ATCC 27294) with inactivation that served as the source of wild type *M. tuberculosis* genomic DNA were purchased from the National Institute for the Control of Pharmaceutical and Biological Products, China.

The preparation of 5′-oligonucleotide-modified Au nanoparticles was performed as reported previously (Goodrich et al., 2004) (Supplemental information; 1).

2.2. Clinical samples and DNA extraction

Thirty-four clinical samples including sputum or urine (n=10) and clinical isolates (n=24) were all collected from Southwest Hospital (Chongqing, China). All were selected from the result of drug-resistance test by BACTEC 460 system (Becton–Dickinson, Spark, MD, USA), resistant to at least isoniazid and rifampin. The sputum samples were firstly liquefied with an equal volume of solution containing 0.5% N-acetylcysteine, 1.45% sodium citrate and 2% NaOH and boiled for 5 min. After centrifugation the precipitate was washed with 0.9% NaCl and resuspended. Clinical isolates were lysed by vortexing a single fresh colony suspended in 90 μL TE buffer (10 mM Tris–HCl, 1 mM EDTA, and pH 7.5) with 50 mg of glass beads (Sigma) (Yao et al., 2010).

2.3. Fabrication of DNA biosensor

The SPR biosensor modified by our laboratory contained a polarized light detection system, a sample-loading chamber, a micro-flow system, a temperature control system and an eight-channel tandem detection well. The sensor chip (20 mm × 28.6 mm) was supplied with a thin gold film layer coated on the upside of glass prism substrate, which formed by the thermal evaporation of gold to an average thickness of 50 nm.

The capture probes were immobilized on the surface of the gold film, which was performed as follows. The gold film of the sensor chip was firstly rinsed with fresh piranha solution for 5 min, then rinsed repeatedly with distilled water and sonicated in ethanol for 5 min, and finally dried with pure nitrogen gas. The immobilization was conducted through the thiol method (Xia et al., 2008). The five capture probes (1 μM) were respectively immobilized to five different channels on the same SPR sensor chip.

2.4. Ligation in solution

Firstly, the PLPs (100 nM) were hybridized with the targets in 20 μL reaction mixture (30 mM Tris–HCl pH 7.8, 4 mM $MgCl_2$, 10 mM $(NH_4)_2SO_4$, 1.2 mM EDTA, and 0.1 mM NAD). It was denatured at 95 °C for 5 min and then cooled down to room temperature (For clinical samples, the genomic DNA was denatured for 5 min in a boiling water bath and then immersed in ice water immediately to wait for hybridization.), and then incubated at 45 °C for 30 min, before 5 U of *E. coli* DNA ligase and 0.05% BSA were added to the mixture and maintained at 37 °C in a water bath for 45 min. Then exonucleolysis was introduced to remove the unligated PLPs and excess linear oligonucleotides. This was performed in 40 μL volume (67 mM glycine-KOH pH 9.5, 6.7 mM $MgCl_2$, and 1 mM DTT) with 10 U of each exonuclease I and exonuclease III. The mixture was incubated at 37 °C for 30 min and terminated by heating at 95 °C for 5 min. Multiplexing was conducted by ligating the targets with the mixture of five PLPs (final concentration 100 nM).

2.5. SPR biosensor real-time monitor

The whole detection procedure was performed under the 650 nm excitation wavelength at 37 °C, and the SPR angle changes were recorded in real time monitoring. Ligation products (circular PLPs) were piped into the detection well in hybridization buffer (0.15 M NaCl, 0.3 M KCl, 10 mM phosphate, 0.005% Tween 20, and pH 7.2) and allowed to anneal for 30 min. Then, the chip surface was thoroughly rinsed by flowing through PBS to remove unhybridized oligonucleotides on the chip surface and residues in the pipeline. After that, 20 μL of RCA reaction mixture (0.5 U uL^{-1} Phi29 DNA polymerase, 1 mM dNTPs, 0.2 μg uL^{-1} BSA, and 5% DMSO) was piped into the detection well and circulated for a period of time with a speed of 5 μL min^{-1}. The resulting solution was piped away by pump to terminate RCA. After equilibrium with PBS for about 3 min, 20 μL of AuNPs with different concentrations was added to incubate for 20 min.

3. Results and discussion

3.1. Probe design

To identify mutations in parallel, the high discriminatory potential of PLP is of primary importance. Each PLP had the similar length of appropriate 85 bp, consisting of four regions: a specific tag-sequence, a general sequence, a restriction endonuclease cutting site and a target-specific region on each detection arm (Fig. 1A). The tag-sequence was composed of five tetramers such that the full length of 20 nucleotide has the similar length and melting temperature (T_m) (60 ± 1 °C), while self-pairing or hairpin formation was eliminated. The circular PLPs containing tag-sequence hybridized with their immobilized anti-tag addresses at 37 °C with minimal crosstalk to each other. Additionally, we adapted asymmetric strategy to design target-specific regions by shortening the 3′ arm-complementary sequence, with a corresponding lengthening of the 5′ arm-complementary sequence (Szemes et al., 2005). Thus the T_m of the 5′ arm of the PLP was 5–10 °C above the ligation temperature (37 °C), while the T_m of 3′ arm was below the ligation temperature. The allele-specific site was positioned at 3′ end of the PLP, which could be strongly discriminated and provided more specificity than that at 5′ end (Luo et al., 1996). This design could increase specificity since it could make an equilibrium process between a bound and unbound 3' arm. We also investigated the nucleotide substitutions (C > A or G > A) within the target-specific region of PLP to circumvent consecutive C or G sequence and decrease the T_m. However, it was found that these substitutions did not noticeably reduce the ligation efficiency, but avoided the secondary structure on the binding arms. The capture probe containing anti-tag sequence with an additional $(T)_{20}$ space linker at its 5′ end improved the accessibility of the DNA hybridization and intensified the signal on the chip surface. Based on the characteristics of the designed probes, we introduced the probe sets into the multiplex detection.

3.2. Principle of the RCA-based SPR multiplex mutations detection

In the RCA-based SPR detection, RCA was performed on the chip surface through the capture probes that acted as an immobilized primer. The detection procedure can be completed by three steps: (i) the PLPs circularization upon the specific recognition of point mutations on DNA targets in solution. (ii) Hybridization of circular PLPs to the capture probes through tag/anti-tag recognition. (iii) Signal amplification by RCA and AuNPs in SPR real-time monitoring (Fig. 1B). Therefore, from measuring the angle change

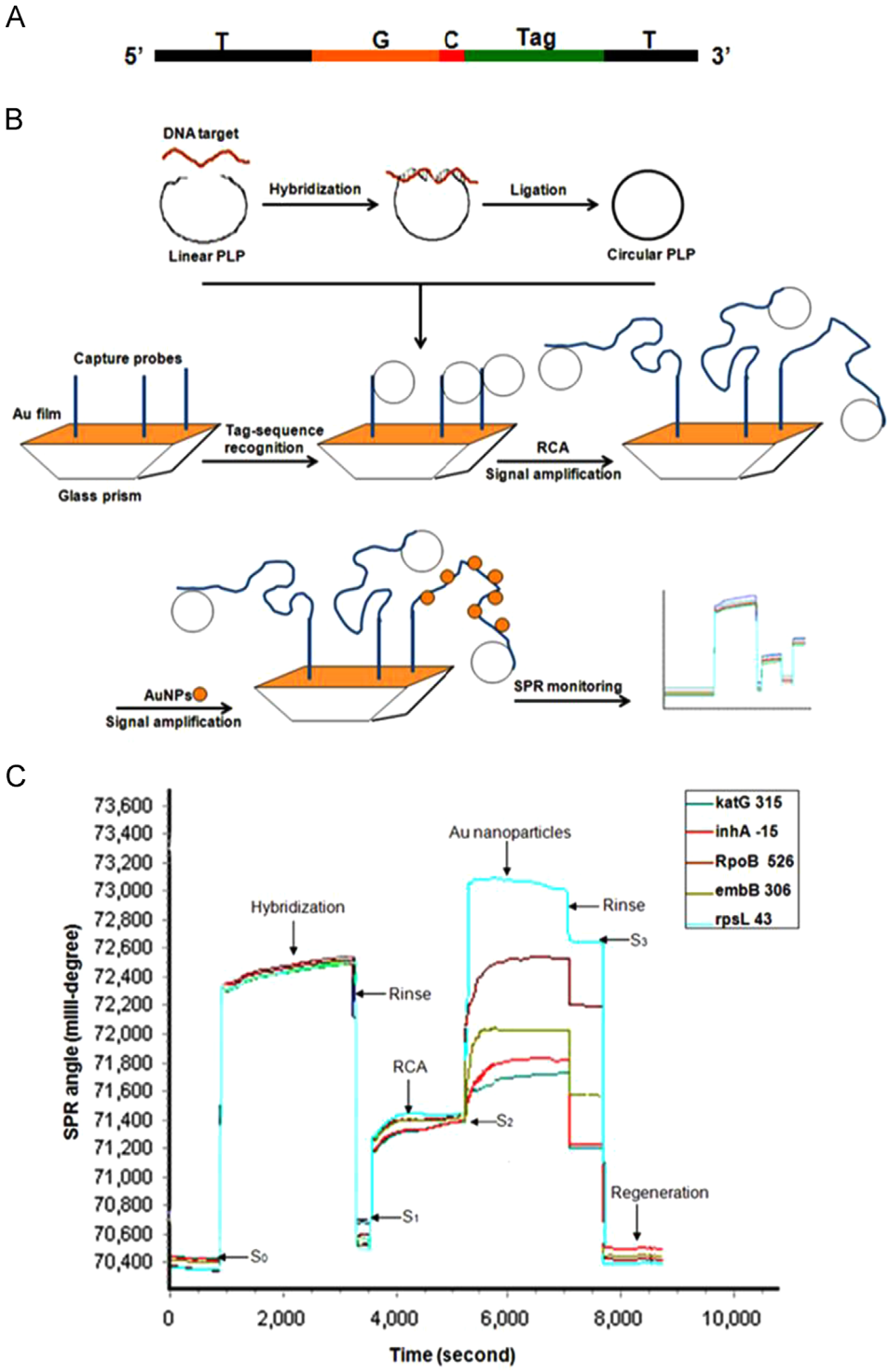

Fig. 1. (A) PLP design. The PLP contains target-complementary sequence (T), general sequence (G) and tag sequence (Tag). Tag sequence is unique for each PLP and complementary to the capture probe immobilized on the chip surface. The general sequence provides the repeats on the RCA products for AuNPs binding. "C" means the cutting site recognized by restriction endonuclease to remove the RCA products from the chip surface after the detection completed. (B) Schematic representation of the proposed detection strategy. (C) Real-time detection of multiple point mutations by SPR sensor.

of SPR biosensor, target sequences could be identified. Furthermore, amplification characteristics could be evaluated continuously with time. Compared with the chip-based ligase-mediated RCA methods, the ligation performed in solution rather than on sensing interface had better specificity and efficiency in mutation discrimination (Melin et al., 2008). By integrating the liquid-phase ligation with the multiplex surface amplification techniques, the proposed method enabled both detection of multiplex mutations in parallel with specificity and amplification of the readout process to improve the sensitivity. The SPR angle change of each step for monitoring the detection of point mutations is shown in Fig. 1C.

3.3. Optimization of experimental conditions

3.3.1. Effect of hybridization temperature

The hybridization between the two termini of PLP and target was the key factor for ensuring the efficiency and specificity of ligation reaction. A suitable hybridization temperature should be determined to minimize the second structure of PLP and assure the full hybridization. A series of hybridization temperatures was evaluated by 10 nM mutant target and 100 nM PLP. As shown in Fig. 2A, the maximum SPR angle change was observed at 45 °C which was close to the T_m of the PLP termini, while the angle change of wild target was always low and changed scarcely. Hence, we set 45 °C as the hybridization temperature for subsequent experiments.

3.3.2. Effect of RCA duration

The duration of RCA was also investigated to obtain higher sensitivity. In this experiment, the RCA duration was varied from 0 to 120 min with an interval of 10 min. The result showed that the SPR angle change was time-determined within the reaction duration, however gradually slowing down when the time went beyond 30 min, as it is shown in Fig. 2B. Since the length of DNA strand generated by RCA was proportional to the RCA duration, one would expect larger signal amplification from longer RCA duration. Furthermore, the longer DNA strand would provide more binding sites for the AuNPs. However, it was found that the duration beyond 30 min did not yield more significant increase of the signal ($p > 0.05$). This might be due to the reason that the entangled RCA products hindered the hybridization with the AuNPs, or that the equilibrium was reached. Therefore, the optimum RCA duration was set as 30 min in the following experiments.

3.3.3. Effect of AuNPs concentration

As a SPR phenomenon based detection, the Au nanoparticles would improve the intrinsic sensitivity of SPR biosensor only when the AuNPs were bound on the chip surface by hybridization with the immobilized RCA products. A suitable AuNPs concentration should favor both the surface refractive index change and the hybridization of AuNPs with the RCA products. As shown in Fig. 2C, the SPR angle change increased with the AuNPs concentration up to 8% (v/v), while the value of wild target was always changed slightly. It might be contributed to the fact that the hybridization reaction has reached saturation level or the augmentation of steric hindrance in the three-dimensional space caused by redundant AuNPs inhibited the hybridization. Moreover, the positive control without AuNPs amplification was also conducted in the same condition. The AuNPs (8% of concentration) enhanced the SPR signal by approximately 2.1-fold compared with the positive control. The magnification was more than the previous study with the nanoparticles of 5 μm diameter (Xia et al., 2008), and less than the diameter of 5 nm (Cai et al., 2011), which meant that the magnification was related to the particle diameter, and the smaller size of nanoparticles would produce larger SPR signal. It demonstrated that the particle–particle separation distance and size would affect the plasmon oscillations with a resonant frequency. Therefore, 8% of AuNPs concentration was chosen as the optimal working concentration.

3.4. Specificity of the RCA-SPR biosensor detection

The specificity of the proposed assay depended on two factors: the ligation reaction in solution and the hybridization reaction on the chip surface. Under the optimized experiment condition, four experiments were carried out to validate the specificity. Fig. 3A

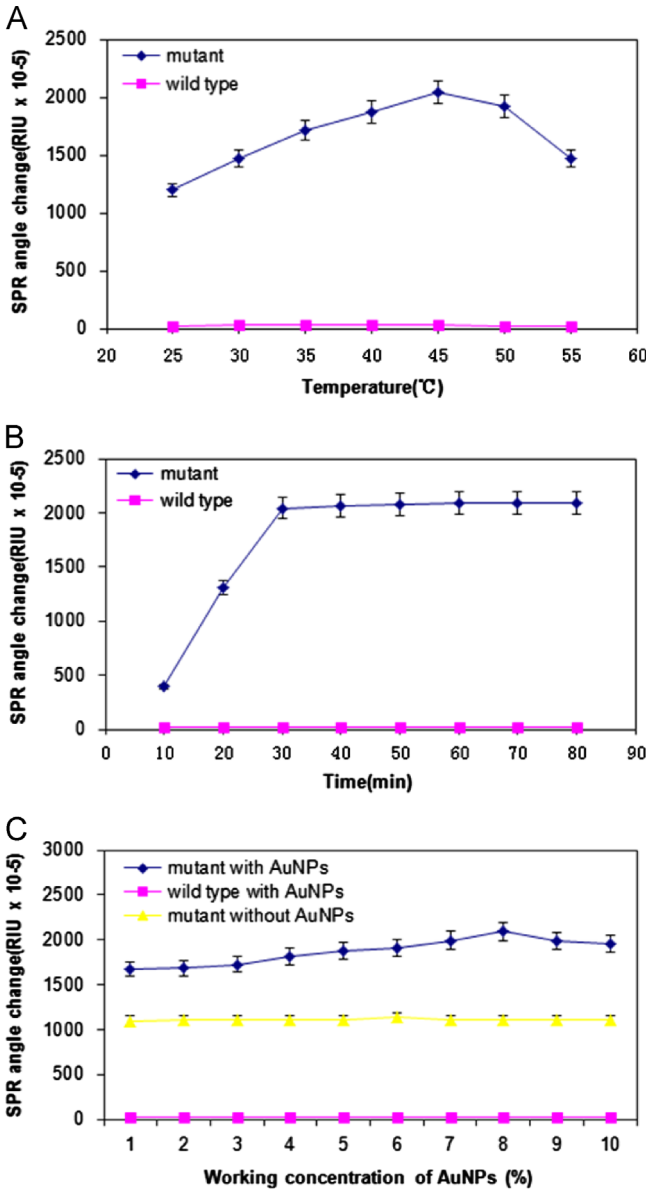

Fig. 2. Optimization of experiment conditions. (A) Hybridization temperature on SPR angle changes. (B) RCA duration on SPR angle changes. (C) AuNPs concentration on SPR angle changes. The concentration of PLP and its perfect-matched target was 100 nM and 10 nM, respectively, in all experiments. RIU indicates refractive index unit, 1millidegree SPR angle = 10^{-5} RIU. Error bars indicate the standard deviation ($n = 5$).

displayed the SPR angle changes from mutant target (red) and wild type target (blue) using the synthesized katG gene sequence with the same concentration of 10 nM. Corresponding control experiments (target-free) were performed under the same procedure as depicted in the experimental section. The angle change for the mutant was $(2031.6 \pm 116.9) \times 10^{-5}$ RIU, which was 104 times higher than that of the wild type (only $(19.5 \pm 5.2) \times 10^{-5}$ RIU) with subtraction of the background value (control). The result demonstrated that when the PLP hybridized with the single-base mismatch target, neither the circularization reaction nor the following amplification reaction occurred. The small angle changes observed from the wild and control was attributed to the limited RCA-free extension from the unligated PLPs.

The ligation reaction in solution was also evaluated by electrophoresis. In Fig. 3B, lane 0 represents the DNA marker (100–1000 bp), lane 1 represents the ligation product from the mutant target, and lanes 2 and 3 represent the ligation products from wild

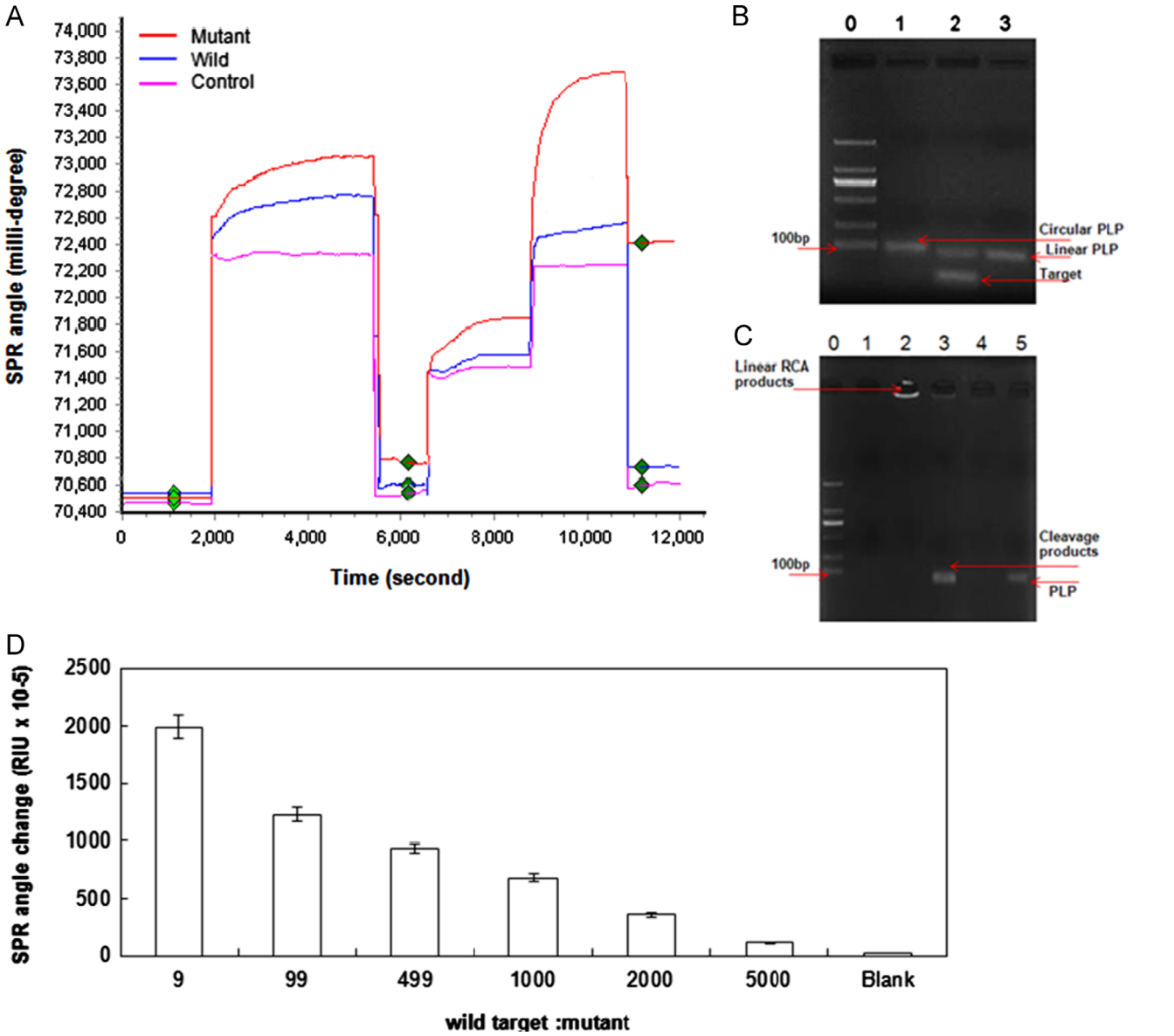

Fig. 3. Specificity investigation. (A) SPR angle values corresponding to mutant target (red), wild type target (blue) and target-free (purple) sample. (B) Electrophoresis identification of the enzymatic ligation reaction. Lanes 1, 2 and 3 represent the ligation products from mutant, wild and target-free samples, respectively. (C) RCA products electrophoresed in 1% agarose gel stained with SYBR Green II dye. Lanes 1 and 4 represent the products from the target-free and wild samples; Lanes 2 and 3 represent the RCA products and RCA-digestion products from mutant target respectively; Lane 5 represents the bands of PLP. (D) Effect of wild target to mutant ratio on the detection of point mutation. Error bars indicate the standard deviation ($n=5$). (For interpretation of the references to color in this figure legend, the reader is referred to the web version of this article.)

target and blank control (target-free), respectively. It was obvious that the linear PLP (83 bp) only circularized in the presence of mutant target, while no ligation products were obtained in the presence of wild target or blank control, which indicated that the ligation reaction was highly specific for discriminating mutant target from wild. Subsequently, the resulting RCA products were electrophoresed in a 1% agarose gel stained with SYBR Green II dye. In Fig. 3C, lanes 2 and 3 represent the RCA products from mutation targets without or with endonuclease digestion, and lanes 1 and 4 represent the RCA products from blank control and wild type targets, respectively. The bands after digestion (lane 3) were of the same size as PLP (lane 5), which meant that the RCA products were long ssDNA composed of multiple tandem repeated copies of the PLP. The results of gel electrophoresis were consistent with that of the SPR assay.

To further evaluate the specificity of our proposed assay, the wild and the mutant targets were mixed together in a total concentration of 100 nM with different mole ratios (9:1, 99:1, 499:1, 1000:1, 2000:1, and 5000:1). The PLP (100 nM) complementary to the mutant target was added. As shown in Fig. 3D, the SPR angle change gradually slowed down with the decrease of mutant target concentration. When the mole ratio was 5000:1 (the mutant target was 20 pM in the mixture), the average SPR angle change was still significantly higher than that of the wild type only ($p<0.05$), indicating that the proposed assay had excellent capability of detecting the low-abundance mutation in the large background of wild targets, which granted the assay great potential in clinical applications.

To investigate the performance of the method in parallel mutation identification, five synthesized mutation target sequences were used to make their complementary linear PLPs circularized. Identification of the different mutation sites into the corresponding channel on chip depended on the specific tag sequence recognition between capture probes and circular PLPs. The cross-reaction was investigated

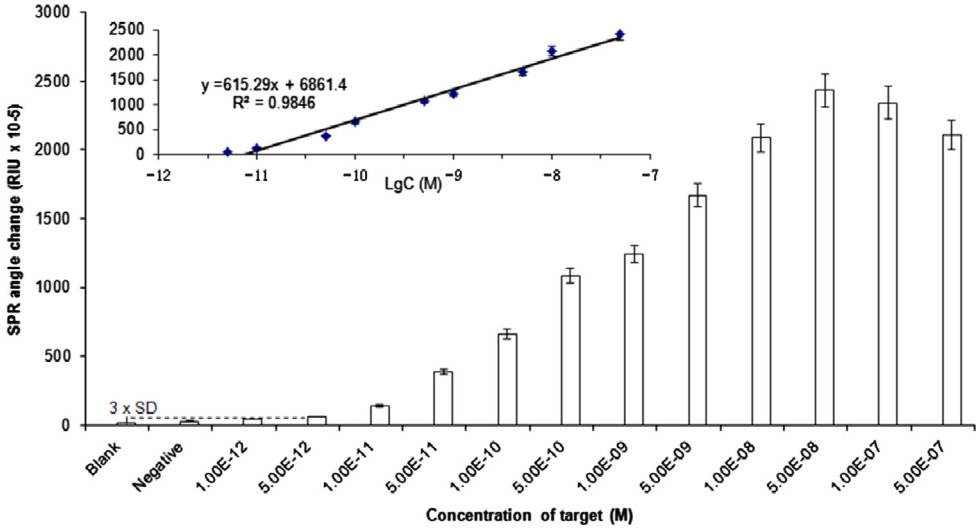

Fig. 4. The sensitivity assessment. The dashed line represents the threshold value. The inset displays the linear relationship between the angle changes vs. log concentration of target sequence. Error bars indicate the standard deviation ($n=5$).

between the circular PLP and the non-specific capture probes to evaluate the selectivity of the method for application to multiplexing detection (Supplemental information; Fig. 1). The differences of SPR angle change were significant between the specific pairs and non-specific pairs ($p<0.01$), which showed great selectivity of the capture probes on the sensor chip. The analysis demonstrated that the cross-reaction between the circular PLP and the non-specific capture probe was very low.

3.5. Sensitivity of the RCA-SPR biosensor detection

With the aforementioned optimizations, the relationship between the SPR angle response and the concentration of mutant target was investigated. The result showed that the SPR angle changes were linear to the logarithm of the target concentration from 10^{-12} M to 10^{-8} M ($y=615.29x+1323.8$, $R^2=0.9846$) (Fig. 4). The detection limit was set at 3-fold standard deviation (SD) more than the blank, so the threshold was determined as $(59.1 \pm 7.1) \times 10^{-5}$ RIU with the concentration of 5×10^{-12} M. The measurements were reproducible for all concentrations with relative standard deviation less than 10% ($n=5$), suggesting an acceptable reproducibility. The SPR angle change increased remarkably with the increase of target DNA concentration, while it increased scarcely when the target DNA increased up to 10^{-7} M. It was probably due to the fact that the PLPs in solution had been completely circularized, or that the high concentration of circular PLPs made the capture probes on chip reach saturation level. The sensitivity of the current assay was comparable or even exceeded the reported similar methods, such as the RCA-based electrochemical assay (0.1 nM) (Zhang et al., 2009); the ligation-mediated colorimetric method (74 pM) (Li et al., 2005); the hybridization detection by SPR biosensor (20 pM) (Milkani et al., 2010) and the SPR method with linker probes (5 nM) (Rachkov et al., 2011). The previous SPR method to detect *M. tuberculosis* without signal amplification had a sensitivity of only 0.05 μM (Duman and Piskin, 2010). In our assay, under the optimum condition, RCA amplified the SPR signal by almost 10-fold before the addition of AuNPs, and the AuNPs enhanced the signal for another approximate 2.1-fold compared with the previous RCA step. Thus, we could conclude that the high sensitivity might be attributed to the signal amplification by the combination of surface-anchored RCA and AuNPs. Firstly, the surface-anchored RCA produced a large ssDNA fragments immobilized on the chip surface to increase the refractive index of the SPR biosensor. Then ssDNA products with thousands of tandem repeats provided a large number of binding sites for AuNPs to hybridize, which enhanced the plasmon oscillation with an intensified resonant frequency, thus making significant improvement to the sensitivity and dynamic range.

Table 2
Comparison of sequencing method and SPR biosensor method for parallel detection of five point mutations.

Sequencing	SPR biosensor										Total
	katG 315		inhA-15		rpoB 526		embB 306		rpsL 43		
	Mut	Wt	Mut	Wt	Mut	Wt	Mut	Wt	Mut	Wt	
Mut	23	1	13	0	17	0	19	0	22	0	
Wt	2	4	0	17	1	12	1	10	0	8	
Total	25	5	13	17	18	12	20	10	23	7	30

Mut: mutant type, and Wt: wild type.

3.6. Detection of clinical samples

We applied this RCA-based SPR multiplexing assay to detect five clinically meaningful point mutations: KatG 315 (AGC→ACC), inhA-15 (ACG→ATG), rpoB 526 (CAC→TAC), embB 306 (ATG→GTG) and rpsL 43 (AAG→AGG) in MDRTB genomic DNA from clinical samples. Each sample was divided into two portions before detection. One portion was used to confirm the genotype by sequencing as a reference method, and the other was used for SPR detection. Several local-specific mutant genotypes which were not targeted by our designed PLPs were excluded (Supplemental information; Table 1). Using the fixed concentration of multiplexing PLPs (100 nM), the detection limit was found to be 8.2 pg μL^{-1} genomic DNA, which was sufficient for detecting clinical samples. However, the detection of *M. tuberculosis* by LAMP was reported with a sensitivity of 5 fg (Aryan et al., 2010). The reaction is primed by three primer pairs leading to exponential amplification, while RCA is a linear amplification reaction. The real-time PCR method also reached a high sensitivity as 10 fg (Wada et al., 2004). Even so, RCA has advantages in resistance to contamination, moderate reaction temperature, multiplex ability, simple reaction schemes, label-free and real-time analysis. In our test, one case of katG mutant type (315 ACC) sample was undetected presumably due to failure of DNA extraction or the paucity of target in the sample. Two cases of wild samples were

inconsistently detected by the SPR method probably due to which the testing DNA was not preserved appropriately leading to contamination before detection (Supplemental information; Table 2). Compared to the sequencing method, the sensitivity and specificity of the SPR detection were 92% and 80%, respectively, for katG 315; 100% and 100%, respectively, for inhA -15; 94.4% and 100%, respectively, for rpoB 526; 95% and 100%, respectively, for embB 306; 100% and 100%, respectively, for rpsL 43 (Table 2). According to the Kappa test, $p < 0.05$, Kappa > 0.75, there exists significant consistency between the two methods.

4. Conclusions

In the present work, we developed a new SPR method for multiplex mutation detection based on surface signal amplification. The high sensitivity and specificity of this method mainly attributed to the high-fidelity of ligation, multiplexing characteristics of probes, amplification potential of surface-anchored RCA and Au nanoparticles, and intrinsically high sensitivity of SPR biosensor. This method exhibited some practical features, such as speed (less than 5 h including DNA extraction), ease of use (entire steps on sensor chip except for the ligation) and low power consumption (isothermal reaction condition).We also demonstrated its application in parallel mutation identification in clinical samples. Five drug-resistance associated point mutations in MDRTB were targeted and identified by the method with good consistency. Future studies will be carried out to improve the multiplexing capabilities of the biosensor array that can target more mutation sites associated with resistance of first and/or second line anti-TB drugs. We eventually hope to extend this platform to the detection of mutations associated with infection disease, hereditary disorders and cancer. However, more detailed work should be done before the clinical application.

Acknowledgments

This study was supported by the grants from the Major Project Chinese National Programs for High Technology Research and Development (863 Program, 2011AA02A121), National Natural Science Foundation of China (30927002, 30970766, and 30901388) and the 12th Five-year-project of Military Funding for Scientific Technology (AWS11C001).

Appendix A. Supporting information

Supplementary data associated with this article can be found in the online version at http://dx.doi.org/10.1016/j.bios.2013.04.044.

References

Aryan, E., Makvandi, M., Farajzadeh, A., Huygen, K., Bifani, P., Mousavi, S.L., Fateh, A., Jelodar, A., Gouya, M.M., Romano, M., 2010. Microbiological Research 165, 211–220.
Bailey, R.C., Qavi, A.J., Washburn, A.L., Byeon, J.Y., 2009. Analytical Chemistry Journals 394, 121–135.
Banér, J., Nilsson, M., Isaksson, A., Mendel-Hartvig, M., Antson, D., Ulf Landegren, U., 2001. Current Opinion in Biotechnology 12, 11–15.
Banér, J., Nilsson, M., Mendel-Hartvig, M., Landegren, U., 1998. Nucleic Acids Research 26, 5073–5078.
Cai, J., Yao, C., Xia, J., Wang, J., Chen, M., Huang, J., Chang, K., Liu, C., Pan, H., Fu, W., 2011. Sensors and Actuators B: Chemical 155, 500–504.
Chu, L.Q., Forch, R., Knoll, W., 2007. Angewandte Chemie, International Edition in English 46, 4944–4947.
Diedrich, C.R., Flynn, J.L., 2011. Infection and Immunity 79, 1407–1417.
Duman, M., Piskin, E., 2010. Biosensors and Bioelectronics 26, 908–912.
Garcia II, B.H., Goodman, R.M., 2008. Journal of Virological Methods 147, 18–25.
Goodrich, G.P., Helfrich, M.R., Overberg, J.J., Keating, C.D., 2004. Langmuir 20, 10246–10251.
Hatch, A., Takeshi, S., Misasi, J., Smith, L.C., 1999. Genetic Analysis: Biomolecular Engineering 15, 35–40.
Homola, J., 2008. Chemical Reviews 108, 462–493.
Jin, W., Lin, X., Lv, S., Zhang, Y., Jin, Q., Mu, Y., 2009. Biosensors and Bioelectronics 24, 1266–1269.
Lee, M.F., Chen, Y.H., Hsu, H.J., Peng, C.F., 2010. Journal of Microbiological Methods 83, 53–58.
Li, J., Chu, X., Liu, Y., Jiang, J.-H., He, Z., Zhang, Z., Shen, G., Yu, R.-Q., 2005. Nucleic Acids Research 33, 168–176.
Lizardi, P.M., Huang, X., Zhu, Z., Bray-Ward, P., Thomas, D.C., Ward, D.C., 1998. Nature Genetics 19, 225–232.
Luo, J., Bergstrom, D.E., Barany, F., 1996. Nucleic Acids Research 24, 3071–3078.
Mannelli, I., Courtois, V., Lecaruyer, P., Roger, G., Millot, M.C., Goossens, M., Canva, M., 2006. Sensors and Acutators B: Chemical 119, 583–591.
Melin, J., Jarvius, J., Larsson, C., Soderberg, O., Landegren, U., Nilsson, M., 2008. New Biotechnology 25, 42–48.
Milkani, E., Morais, S., Lambert, C.R., McGimpsey, W.G., 2010. Biosensors and Bioelectronics 25, 1217–1220.
Mitchell, J.S., Lowe, T.E., 2009. Biosensors and Bioelectronics 24, 2177–2183.
Niu, S., Jiang, Y., Zhang, S., 2010. Chemical Communications 46, 3089–3091.
Petryayeva, E., Krull, U.J., 2011. Analytica Chimica Acta 706, 8–24.
Rachkov, A., Patskovsky, S., Soldatkin, A., Meunier, M., 2011. Talanta 85, 2094–2099.
Ramaswamy, S., Musser, J.M., 1998. Tuberculosis 79, 3–29.
Schweitzer, B., Kingsmore, S., 2001. Current Opinion in Biotechnology 12, 21–27.
Szemes, M., Bonants, P., de Weerdt, M., Baner, J., Landegren, U., Schoen, C.D., 2005. Nucleic Acids Research 33, 70–82.
Veigas, B., Machado, D., Perdigao, J., Portugal, I., Couto, I., Viveiros, M., Baptista, P.V., 2010. Nanotechnology 21, 1–7.
Wada, T., Maeda, S., Tamaru, A., Imai, S., Hase, A., Kobayashi, K., 2004. Journal of Clinical Microbiology 42, 5277–5285.
Wang, J., Luo, Y., Zhang, B., Chen, M., Huang, J., Zhang, K., Gao, W., Fu, W., Jiang, T., Liao, P., 2011. Journal of Translation Medicine 9, 85–93.
Wang, S., Yang, H., Zhang, H., Yang, F., Zhou, M., Jia, C., Lan, Y., Ma, Y., Zhou, L., Tian, S., Wang, S., Zhang, H., Chen, Z., 2010. Cancer Genetics and Cytogenetics 200, 100–105.
World Health Organization, 2012. , Global Tuberculosis Report 2012. http://www.who.int/tb/publications/global_report/en/index.html.
Xia, H., Wang, F., Huang, Q., Huang, J., Chen, M., Wang, J., Yao, C., Chen, Q., Cai, G., Fu, W., 2008. Sensors 8, 6453–6470.
Yao, C., Zhu, T., Li, Y., Zhang, L., Zhang, B., Huang, J., Fu, W., 2010. Clinical Microbiology and Infection 16, 1639–1643.
Zhang, S., Wu, Z., Shen, G., Yu, R., 2009. Biosensors and Bioelectronics 24, 3201–3207.
Zhong, X.B., Lizardi, P.M., Huang, X.H., Bray-Ward, P.L., Ward, D.C., 2001. Proceedings of the National Academy of Sciences, USA 98, 3940–3945.